

See discussions, stats, and author profiles for this publication at: <https://www.researchgate.net/publication/26798416>

# Controlled Delivery Systems Using Antibody-Capped Mesoporous Nanocontainers

ARTICLE in JOURNAL OF THE AMERICAN CHEMICAL SOCIETY · OCTOBER 2009

Impact Factor: 12.11 · DOI: 10.1021/ja904456d · Source: PubMed

CITATIONS

151

READS

102

10 AUTHORS, INCLUDING:



Ramón Martínez-Máñez

Universitat Politècnica de València

339 PUBLICATIONS 11,684 CITATIONS

SEE PROFILE



Angel Maquieira

Universitat Politècnica de València

208 PUBLICATIONS 3,569 CITATIONS

SEE PROFILE



Rosa Puchades

Universitat Politècnica de València

185 PUBLICATIONS 3,098 CITATIONS

SEE PROFILE



Pedro Amorós

University of Valencia

220 PUBLICATIONS 4,946 CITATIONS

SEE PROFILE

## Controlled Delivery Systems Using Antibody-Capped Mesoporous Nanocontainers

Estela Climent,<sup>†,‡</sup> Andrea Bernardos,<sup>†</sup> Ramón Martínez-Máñez,<sup>\*,†,‡</sup>  
 Angel Maquieira,<sup>\*,†</sup> Maria Dolores Marcos,<sup>†,‡</sup> Nuria Pastor-Navarro,<sup>†</sup>  
 Rosa Puchades,<sup>†</sup> Félix Sancenón,<sup>†,‡</sup> Juan Soto,<sup>†,‡</sup> and Pedro Amorós<sup>\*,§</sup>

*Instituto de Reconocimiento Molecular y Desarrollo Tecnológico, Centro Mixto Universidad Politécnica de Valencia–Universidad de Valencia, Valencia, Spain, Departamento de Química, Universidad Politécnica de Valencia, Camino de Vera s/n 46022, Valencia, Spain, Centro Investigación Biomédica en Red de Bioingeniería, Biomateriales y Nanomedicina, and Institut de Ciència del Materials, Universitat de València, Post Office Box 2085, E-46071 València, Spain*

Received June 3, 2009; E-mail: rmaez@qim.upv.es; amaqueira@qim.upv.es; pedro.amoros@uv.es

**Abstract:** This paper describes the design of new controlled delivery systems consisting of a mesoporous support functionalized on the pore outlets with a certain hapten able to interact with an antibody that acts as a nanoscopic cap. The opening protocol and delivery of the entrapped guest is related by a displacement reaction involving the presence in the solution of the antigen to which the antibody is selective. As a proof-of-the-concept, the solid MCM-41 was selected as support and was loaded with the dye [Ru(bipy)<sub>3</sub>]Cl<sub>2</sub>. Then a suitable derivative of the hapten 4-(4-aminobenzenesulfonylamino)benzoic acid was anchored on the outer surface of the mesoporous support (solid **S1**). Finally the pores were capped with a polyclonal antibody for sulfathiazole (solid **S1-AB**). Delivery of the dye in the presence of a family of sulfonamides was studied in phosphate-buffered saline (PBS; pH 7.5). A selective uncapping of the pores and dye delivery was observed for sulfathiazole. This delivery behavior was compared with that shown by other solids that were prepared as models to assess the effect of the hapten and its interaction with antibody in the dye delivery control in the presence of the antigen.

### Introduction

Among the large amount of approximations toward the development of new smart materials, one particularly tempting is the possibility to create stimuli-responsive nanosolids able to react to environmental changes or showing switchable behaviors.<sup>1,2</sup> One appealing application of such systems is the design of functionalized nanocontainers able to deal with cargo delivery under controlled conditions via external triggers.<sup>3</sup> Traditional delivery systems usually rely on simple diffusion-controlled processes or degradation of the nanocarrier,<sup>4</sup> using for instance microcapsules,<sup>5</sup> micelles,<sup>6</sup> vesicles,<sup>7</sup> or liposomes.<sup>8</sup> As an alternative to these materials, silica mesoporous supports

(SMPS) show unique properties such as large load capacity, biocompatibility, high thermal stability, homogeneous porosity, inertness, and tunable pore sizes with a diameter of ca. 2–10 nm.<sup>9</sup> Moreover, it has been recently demonstrated that it is possible to incorporate in the external surface of SMPS functional groups able to be opened or closed at will for functional control release applications. Specifically, it has been

<sup>†</sup> Instituto de Reconocimiento Molecular y Desarrollo Tecnológico, Centro Mixto Universidad Politécnica de Valencia–Universidad de Valencia, and Departamento de Química, Universidad Politécnica de Valencia.

<sup>‡</sup> CIBER de Bioingeniería, Biomateriales, y Nanomedicina.

<sup>§</sup> Institut de Ciència dels Materials, Universitat de València.

- (1) Ariga, K.; Vinu, A.; Hill, J. P.; Mori, T. *Coord. Chem. Rev.* **2007**, *251*, 2562.
- (2) Katz, E.; Willner, I. *Angew. Chem., Int. Ed.* **2004**, *43*, 6042.
- (3) Descalzo, A. B.; Martínez-Máñez, R.; Sancenón, F.; Hoffmann, K.; Rurack, K. *Angew. Chem., Int. Ed.* **2006**, *45*, 5924–5948.
- (4) (a) Puoci, F.; Iemma, F.; Picci, N. *Curr. Drug Delivery* **2008**, *5*, 85–96. (b) Siepmann, F.; Siepmann, J.; Walther, M.; MacRae, R.; Bodmeier, R. *J. Controlled Release* **2008**, *125*, 1–15.
- (5) Hamidi, M.; Azadi, A.; Rafiei, P. *Adv. Drug Delivery Rev.* **2008**, *17*, 1638.
- (6) Pouton, C. W.; Porter, C. J. H. *Adv. Drug Delivery Rev.* **2008**, *17*, 625.
- (7) Rijcken, C. J. F.; Soga, O.; Hennink, W. E.; van Nostrum, C. F. J. *Controlled Release* **2007**, *120*, 131.

- (8) Andresen, T. L.; Jensen, S. S.; Jorgensen, K. *Prog. Lipid Res.* **2005**, *44*, 69.
- (9) (a) Beck, J. S.; Vartuli, J. C.; Roth, W. J.; Leonowicz, M. E.; Kresge, C. T.; Schmitt, K. D.; Chu, C. T.-W.; Olson, D. H.; Sheppard, E. W.; McCullen, S. B.; Higgins, J. B.; Schlenker, J. L. *J. Am. Chem. Soc.* **1992**, *114*, 10834–10843. (b) Wright, A. P.; Davis, M. E. *Chem. Rev.* **2002**, *102*, 3589–3614. (c) Kikelbick, G. *Angew. Chem., Int. Ed.* **2004**, *43*, 3102–3104. (d) Stein, A. *Adv. Mater.* **2003**, *15*, 763–775.
- (10) (a) Casasús, R.; Marcos, M. D.; Martínez-Máñez, R.; Ros-Lis, J. V.; Soto, J.; Villaescusa, L. A.; Amorós, P.; Beltrán, D.; Guillem, C.; Latorre, J. *J. Am. Chem. Soc.* **2004**, *126*, 8612–8613. (b) Casasús, R.; Climent, E.; Marcos, M. D.; Martínez-Máñez, R.; Sancenón, F.; Soto, J.; Amorós, P.; Cano, J.; Ruiz, E. *J. Am. Chem. Soc.* **2008**, *130*, 1903–1917. (c) Bernardos, A.; Aznar, E.; Coll, C.; Martínez-Máñez, R.; Barat, J. M.; Marcos, M. D.; Sancenón, F.; Soto, J. *J. Controlled Release* **2008**, *131*, 181–189. (d) Yang, Q.; Wang, S.; Fan, P.; Wang, L.; Di, Y.; Lin, K.; Xiao, F.-S. *Chem. Mater.* **2005**, *17*, 5999–6003. (e) Nguyen, T. D.; Leung, K. C.-F.; Liong, M.; Pentecost, C. D.; Stoddart, J. F.; Zink, J. I. *Org. Lett.* **2006**, *8*, 3363–3366. (f) Leung, K. C.-F.; Nguyen, T. D.; Stoddart, J. F.; Zink, J. I. *Chem. Mater.* **2006**, *18*, 5919–5928. (g) Angelos, S.; Yang, Y.-W.; Patel, K.; Stoddart, J. F.; Zink, J. I. *Angew. Chem., Int. Ed.* **2008**, *47*, 2222–2226. (h) Khashab, N. M.; Trabolsi, A.; Lau, Y. A.; Ambrogio, M. W.; Friedman, D. C.; Khatib, H. A.; Zink, J. I.; Stoddart, J. F. *Eur. J. Org. Chem.* **2009**, 1669–1673. (i) Park, C.; Oh, K.; Lee, S. C.; Kim, C. *Angew. Chem., Int. Ed.* **2007**, *46*, 1455–1457.

reported that it is possible to design systems able to achieve zero release, which can be fully opened on command via external physical or chemical stimuli. Recently, SMPS-based systems displaying controlled release have been reported that contain different caps such as nanoparticles, nanovalves, and supramolecular frameworks that in most cases use changes in pH,<sup>10</sup> temperature,<sup>11</sup> redox potential,<sup>12,13</sup> or light<sup>14</sup> or rely in the presence of small molecules<sup>15</sup> for uncapping the pores.

Despite these examples, the use of SMPS equipped with gatelike scaffolds for the preparation of real delivery systems is still in its infancy. Thus, in relation to gated systems, some examples still show disadvantages for their potential use in advanced applications such as lack of operational features in aqueous environments, use of difficult-to-apply or complex stimuli, etc. In particular, regardless of very recent reported gated SMPS that can be uncapped by enzymes<sup>16</sup> or can be controlled

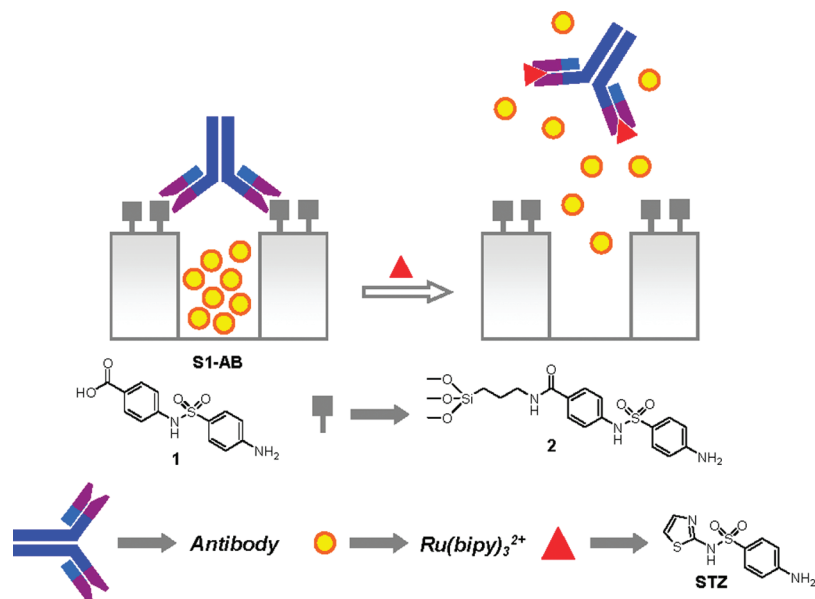
by certain carbohydrates,<sup>17</sup> there is an almost complete lack of SMPS-based devices designed to trigger cargo release involving biomolecules. In order to advance in this field and as a proof-of-the-concept, we were interested in demonstrating that antibody–antigen interaction could be a powerful switchable method to develop tailor-made SMPS for controlled delivery functions. In particular, and as a part of our interest in the use of inorganic supports for advanced applications,<sup>18</sup> we report here the design of a new controlled delivery system consisting of a mesoporous support functionalized on the pore outlets with a certain hapten able to be recognized by an antibody that acts as a nanoscopic cap. The opening protocol and delivery of the entrapped guest is related to a highly effective displacement reaction involving the presence in the solution of the antigen to which the antibody is selective.

## Results and Discussion

**Design and Synthesis of the Gated Material.** As stated above, the incorporation of gatelike ensembles on mesoporous scaffolds has proved to be a suitable approach for the development of nanoscopic solids for mass transport control and for studying the factors that could influence the design of gating functions. Apart from molecular and supramolecular models used for the design of gated supports, we were particularly interested in designing systems where delivery could be governed by biomolecules. Thus, our attention was focused on the specific interaction between antibodies and antigens.<sup>19</sup>

The proposed paradigm is depicted in Scheme 1. In this approach, the external surface of a suitable SMPS is first functionalized with a hapten (solid **S1**) and then the mesopores are capped with a certain antibody that shows good affinity and selectivity toward the anchored hapten via suitable interaction through the two binding IgG regions of the former (solid **S1-AB**). It was expected that the typical size of antibodies (ca. 5.5 nm)<sup>20</sup> would be enough to cap the mesopores in the SMPS. As illustrated in Scheme 1, the presence in the solution of the corresponding antigen (complementary to the antibody) would induce the uncapping of the pores and release of the entrapped guest. In order to study the functional open/close protocol of the gated ensemble, the dye [Ru(bipy)<sub>3</sub>]<sup>2+</sup> was loaded on the inner mesopores of the MCM-41 solid. Thus, the state of the gatelike system is easily monitored via the emission band of the [Ru(bipy)<sub>3</sub>]<sup>2+</sup> dye at  $\lambda = 610$  nm ( $\lambda_{\text{ex}} = 453$  nm) in the aqueous phase. Following this procedure, the solid for delivery studies was prepared with MCM-41 solid as the SMPS and sulfathiazole (STZ) as the antigen. Polyclonal sera for STZ were obtained for this target by immunization of female New Zealand rabbits with bovine serum albumin (BSA)–protein conjugates

- (11) Fu, Q.; Rao, G. V. R.; Ista, L. K.; Wu, Y.; Andrzejewski, B. P.; Sklar, L. A.; Ward, T. L.; López, G. P. *Adv. Mater.* **2003**, *15*, 1262.
- (12) (a) Trewyn, B. G.; Giri, S.; Slowing, I. I.; Lin, V. S.-Y. *Chem. Commun.* **2007**, 3236–3245. (b) Trewyn, B. G.; Slowing, I. I.; Giri, S.; Chen, H.-T.; Lin, V. S.-Y. *Acc. Chem. Res.* **2007**, *40*, 846–853. (c) Lai, C.-Y.; Trewyn, B. G.; Jeftinija, D. M.; Jeftinija, K.; Xu, S.; Jeftinija, S.; Lin, V. S.-Y. *J. Am. Chem. Soc.* **2003**, *125*, 4451–4459. (d) Torney, F.; Trewyn, B. G.; Lin, V. S.-Y.; Wang, K. *Nat. Nanotechnol.* **2007**, *2*, 295–300. (e) Radu, D. R.; Lai, C.-Y.; Jeftinija, K.; Rowe, E. W.; Jeftinija, S.; Lin, V. S.-Y. *J. Am. Chem. Soc.* **2004**, *126*, 13216–13217. (f) Giri, S.; Trewyn, B. G.; Stellmaker, M. P.; Lin, V. S.-Y. *Angew. Chem., Int. Ed.* **2005**, *44*, 5038–5044. (g) Slowing, I. I.; Trewyn, B. G.; Lin, V. S.-Y. *J. Am. Chem. Soc.* **2007**, *129*, 8845–8849. (h) Slowing, I. I.; Trewyn, B. G.; Giri, S.; Lin, V. S.-Y. *Adv. Funct. Mater.* **2007**, *17*, 1225–1236. (i) Montera, R.; Vivero-Escoto, J.; Slowing, I. I.; Garrone, E.; Onida, B.; Lin, V. S.-Y. *Chem. Commun.* **2009**, 3219–3221.
- (13) (a) Zhao, Y.; Trewyn, B. G.; Slowing, I. I.; Lin, V. S.-Y. *J. Am. Chem. Soc.* **2009**, *131*, 8398–8400. (b) Hernandez, R.; Tseng, H.-R.; Wong, J. W.; Stoddart, J. F.; Zink, J. I. *J. Am. Chem. Soc.* **2004**, *126*, 3370–3371. (c) Nguyen, T. D.; Tseng, H.-R.; Celeste, P. C.; Flood, A. H.; Liu, Y.; Stoddart, J. F.; Zink, J. I. *Proc. Natl. Acad. Sci. U.S.A.* **2005**, *102*, 10029–10034. (d) Nguyen, T. D.; Liu, Y.; Saha, S.; Leung, K. C.-F.; Stoddart, J. F.; Zink, J. I. *J. Am. Chem. Soc.* **2007**, *129*, 626–634. (e) Nguyen, T. D.; Leung, K. C.-F.; Liang, M.; Liu, Y.; Stoddart, J. F.; Zink, J. I. *Adv. Funct. Mater.* **2007**, *17*, 2101–2110. (f) Fujiwara, M.; Terashima, S.; Endo, Y.; Shiokawa, K.; Ohue, H. *Chem. Commun.* **2006**, 4635–4637. (g) Liu, R.; Zhao, X.; Wu, T.; Feng, P. *J. Am. Chem. Soc.* **2008**, *130*, 14418–14419.
- (14) (a) Mal, N. K.; Fujiwara, M.; Tanaka, Y. *Nature* **2003**, *421*, 350–353. (b) Mal, N. K.; Fujiwara, M.; Tanaka, Y.; Taguchi, T.; Matsukata, M. *Chem. Mater.* **2003**, *15*, 3385–3394. (c) Zhu, Y.; Fujiwara, M. *Angew. Chem., Int. Ed.* **2007**, *46*, 2241–2244. (d) Lu, J.; Choi, E.; Tamanoi, F.; Zink, J. I. *Small* **2008**, *4*, 421–426. (e) Angelos, S.; Choi, E.; Vögtle, F.; De Cola, L.; Zink, J. I. *J. Phys. Chem. C* **2007**, *111*, 6589–6592. (f) Liu, N.; Dunphy, D.; Atanassov, P.; Bunge, S. D.; Chen, Z.; López, G. P.; Boyle, T. J.; Brinker, C. J. *Nano Lett.* **2004**, *4*, 551–554. (g) Ferris, D. P.; Zhao, Y.-L.; Khashab, N. M.; Khatib, H. A.; Stoddart, J. F.; Zink, J. I. *J. Am. Chem. Soc.* **2009**, *131*, 1686–1688. (h) Aznar, E.; Casasús, R.; García-Acosta, B.; Marcos, M. D.; Martínez-Máñez, R.; Sancenón, F.; Soto, J.; Amorós, P. *Adv. Mater.* **2007**, *19*, 2228–2231. (i) Vivero-Escoto, J. L.; Slowing, I. I.; Wu, C.-Y.; Lin, V. S.-Y. *J. Am. Chem. Soc.* **2009**, *131*, 3462–3463. (j) Aznar, E.; Marcos, M. D.; Martínez-Máñez, R.; Sancenón, F.; Soto, J.; Amorós, P.; Guillem, C. *J. Am. Chem. Soc.* **2009**, *131*, 6833–6843.
- (15) (a) Coll, C.; Casasús, R.; Aznar, E.; Marcos, M. D.; Martínez-Máñez, R.; Sancenón, F.; Soto, J.; Amorós, P. *Chem. Commun.* **2007**, 1957–1959. (b) Casasús, R.; Aznar, E.; Marcos, M. D.; Martínez-Máñez, R.; Sancenón, F.; Soto, J.; Amorós, P. *Angew. Chem., Int. Ed.* **2006**, *45*, 6661–6664. (c) Aznar, E.; Coll, C.; Marcos, M. D.; Martínez-Máñez, R.; Sancenón, F.; Soto, J.; Amorós, P.; Cano, J.; Ruiz, E. *Chem.—Eur. J.* **2009**, *15*, 6877–6888.
- (16) (a) Patel, K.; Angelos, S.; Dichtel, W. R.; Coskun, A.; Yang, Y.-W.; Zink, J. I.; Stoddart, J. F. *J. Am. Chem. Soc.* **2008**, *130*, 2382–2383. (b) Schlossbauer, A.; Kecht, J.; Bein, T. *Angew. Chem., Int. Ed.* **2009**, *48*, 3092–3095. (c) Bernardos, A.; Aznar, E.; Marcos, M. D.; Martínez-Máñez, R.; Sancenón, F.; Soto, J.; Barat, J. M.; Amorós, P. *Angew. Chem., Int. Ed.* **2009**, *48*, 5884–5887.
- (17) Zhao, Y.; Trewyn, B. G.; Slowing, I. I.; Lin, V. S.-Y. *J. Am. Chem. Soc.* **2009**, *131*, 8398–8400.
- (18) See for instance: (a) Climent, E.; Calero, P.; Marcos, M. D.; Martínez-Máñez, R.; Sancenón, F.; Soto, J. *Chem.—Eur. J.* **2009**, *15*, 1816–1820. (b) Ros-Lis, J. V.; Casasús, R.; Comes, M.; Coll, C.; Marcos, M. D.; Martínez-Máñez, R.; Sancenón, F.; Soto, J.; Amorós, P.; El Haskouri, J.; Garró, N.; Rurack, K. *Chem.—Eur. J.* **2008**, *14*, 8267–8278. (c) Comes, M.; Marcos, M. D.; Martínez-Máñez, R.; Sancenón, F.; Soto, J.; Villacusa, L. A.; Amorós, P. *Chem. Commun.* **2008**, 3639–3641. (d) Calero, P.; Aznar, E.; Lloris, J. M.; Marcos, M. D.; Martínez-Máñez, R.; Ros-Lis, J. V.; Soto, J.; Sancenón, F. *Chem. Commun.* **2008**, 1668–1670.
- (19) Diamandis, E. P.; Christopoulos, T. K. Eds.; *Immunoassay*; Academic Press: San Diego, CA, 1996.
- (20) (a) Silverton, E. W.; Navia, M. A.; Davies, D. R. *Proc. Natl. Acad. Sci. U.S.A.* **1977**, *74*, 5140–5144. (b) Francis, G. E., Delgado, C., Eds.; *Methods in Molecular Medicine, Vol. 25. Drug Targeting: Strategies, Principles, and Applications*; Humana Press, Inc.: Totowa, NJ, 2007.

**Scheme 1.** Schematic Representation of Gated Material **S1** Capped with Antibody and Structures of Hapten **1**, Hapten Derivative **2**, and the Antigen Sulfathiazole (STZ)

containing the hapten **1**. The same hapten **1** was made to react with 3-aminopropyltrimethoxysilane to furnish **2**, which was anchored on the SMPS surface in order to prepare **S1** (see Supporting Information for details).<sup>21</sup>

Solid **S1** should ideally contain the hapten **1** anchored on the external surface, whereas the dye must be contained in the mesopore channels. Given that in mesoporous systems the inner surface is much larger than the external, the preparation of the solid should be carried out in a programmed fashion. To prepare the organized hybrid material **S1** we made use of a two-step synthetic procedure that has been used recently by other authors and by us to develop responsive gating structures containing a certain cargo in the pores and suitable switchable ensembles on the pore outlets.<sup>15,16c</sup> Thus, in a first step, the mesoporous starting scaffold was added to a solution containing a relatively high concentration of  $[\text{Ru}(\text{bipy})_3]^{2+}$  dye in order to achieve efficient loading of the pores. Then in the same mixture the hapten derivative **2** was added. This is expected to result in final solids where **2** is basically placed on the external surface of the mesoporous silica-based scaffolding because the anchoring reaction of **2** is carried out when the pores are filled with the ruthenium dye. The final yellow/orange solid (**S1**) was filtered, washed with acetonitrile, and dried at 40 °C for 12 h.

For preparation of the final gated material (**S1-AB**), 400  $\mu\text{g}$  of the SMPS **S1** was suspended in 400  $\mu\text{L}$  of a solution containing the antibody in phosphate-buffered saline (PBS, pH 7.5; see Supporting Information for the exact composition). Optimization of the conditions was performed by checking board titrations with several sera and a range of different serum dilutions (see Supporting Information). **S1-AB** was isolated by centrifugation and washed with PBS to eliminate the residual dye and the free antibody.

For the sake of comparison, and as control supports, two additional solids were prepared. One (**S2**) is a material containing only the  $[\text{Ru}(\text{bipy})_3]^{2+}$  dye on the pore voids, whereas the other (**S3**) contains  $[\text{Ru}(\text{bipy})_3]^{2+}$  on the mesopores and polyamines on the external surface (see Supporting Information).

This second solid, containing amines, was expected to display some interaction with the antibody because sulfathiazole (for which the antibody is selective) also contains an amino group. Both solids will allow assessing the effect that the hapten grafted onto the MCM-41 pores and its interaction with the antibody has in the dye delivery control in the presence of antigen. The procedure to obtain **S2** was the same as described for **S1** but without grafting the hapten **2** on the external surface. Additionally **S3** was prepared, following literature procedures by reaction of dye-loaded MCM-41 with 3-[2-(2-aminoethylamino)ethylamino]propyltrimethoxysilane (**3**) (see Supporting Information).<sup>15b</sup>

**Characterization of Materials.** Solid **S1** was characterized by standard procedures. Figure 1 shows powder X-ray diffraction (PXRD) patterns of the MCM-41 support and the **S1** functionalized material. The PXRD of siliceous MCM-41 as synthesized (curve a) shows four low-angle reflections typical of a hexagonal array. A significant displacement of the (100) peak in the PXRD powder of the MCM-41 calcined sample (curve b) is clearly appreciated due to condensation of silanol groups during the calcination step. Finally, curve c corresponds to the **S1** PXRD pattern. In this case, all reflections except (100) are lost, most likely related to a change of contrast due to the filling of the pore voids with the ruthenium(II) dye. The value and intensity of the (100) peak in this pattern is strong evidence that the loading process with the dye and the further functionalization with hapten have not damaged the mesoporous scaffolding. The presence of the mesoporous structure in the MCM-41 calcined sample and final functionalized solids is also observed by TEM analysis, in which the typical hexagonal porosity of the MCM-41 matrix can be seen (see Figure 1).

The  $\text{N}_2$  adsorption–desorption isotherms of the MCM-41 calcined material show a typical type IV isotherm in which the observed step can be related to the nitrogen condensation inside the mesopores by capillarity. The absence of a hysteresis loop in this interval and the narrow pore distribution suggest the existence of uniform cylindrical mesopores. Application of the BET model resulted in a value for the total specific surface of 1246  $\text{m}^2/\text{g}$ . The  $\text{N}_2$  adsorption–desorption isotherm of **S1** is

(21) Langone, J.; van Vunakis, H. *Methods Enzymol.* **1982**, *84*, 628–640.



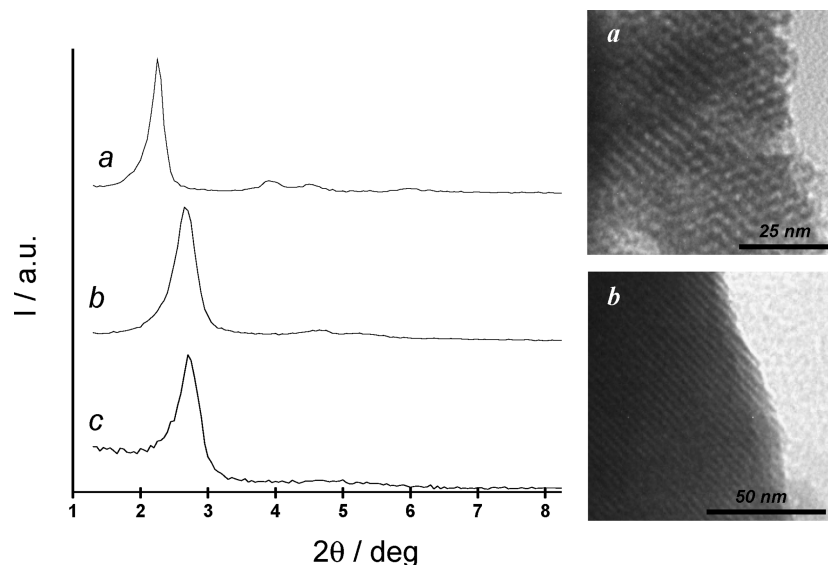


**Figure 1.** (Left) Powder X-ray patterns of the solids (a) MCM-41 as synthesized, (b) calcined MCM-41, and (c) **S1** containing the dye  $[\text{Ru}(\text{bipy})_3]^{2+}$  and hapten derivative **2**. (Right) TEM images of (a) calcined MCM-41 sample and (b) solid **S1**, showing the typical hexagonal porosity of the MCM-41 mesoporous matrix.

**Table 1.** BET Specific Surface Values, Pore Volumes, and Pore Sizes Calculated from  $\text{N}_2$  Adsorption–Desorption Isotherms<sup>a</sup> for Selected Materials

	$S_{\text{BET}}$ ( $\text{m}^2/\text{g}$ )	pore volume <sup>a</sup> ( $\text{cm}^3/\text{g}$ )	pore size <sup>a</sup> (nm)
MCM-41	1246	0.85	2.39
<b>S1</b>	291	0.22	2.31
<b>S3</b>	110	0.35	2.18

<sup>a</sup> Volume ( $V$ ) and diameter ( $D$ ) of mesopore.

**Table 2.** Content ( $\alpha$ ) of Hapten Derivative **2** in **S1**, Polyamine in **S3**, and Dye in Prepared Solids

solid	$\alpha_{\text{hapten } 2}$ (mmol/g of $\text{SiO}_2$ )	$\alpha_{\text{polyamine}}$ (mmol/g of $\text{SiO}_2$ )	$\alpha_{\text{dye}}$ (mmol/g of $\text{SiO}_2$ )
<b>S1</b>	0.38		0.66
<b>S1-AB</b>	0.38		0.12
<b>S2</b>			0.69
<b>S3</b>		0.40	0.60
<b>S3-AB</b>		0.40	0.15

typical of mesoporous systems with filled mesopores, and a significant decrease in the  $\text{N}_2$  volume adsorbed is observed (see Supporting Information). In fact, this solid presents relatively flat curves when compared (at the same scale) to the MCM-41 material, indicating that there is significant pore blocking. Similar results have been observed for the parent solid **S3** and by us in related systems. BET specific surface values, pore volumes, and pore sizes calculated from the  $\text{N}_2$  adsorption–desorption isotherms for MCM-41 and **S1** and **S3** are listed in Table 1 (see Supporting Information for more details).

The content of hapten derivative **2** in **S1**, polyamine in **S3**, and dye in prepared solids, determined by elemental analysis and thermogravimetric and delivery studies, is shown in Table 2. Further detail for the synthesis and characterization of **S3** is included in Supporting Information.

When the amount of STZ that induced the observed dye release is taken into account, and with the assumption that two molecules of STZ interact with one antibody molecule (if total occupation is supposed), it can be estimated that **S1-AB** material contains  $1.74 \times 10^{18}$  antibody molecules/g of solid. Additionally,

from the typical external surface for a MCM-41 support, this results in an average distance between antibodies of ca. 7.6 nm, a value that is in agreement with the typical effective antibody molecular radius of 5.5 nm. Moreover, from the antibody and hapten contents, a ratio of 86 hapten molecules/antibody molecules was estimated.

**Functional Antigen-Driven Controlled Release.** As stated above, we aimed to design delivery systems triggered by a certain antigen by use of antibody-capped mesoporous scaffolds. The uncapping protocol, that is, delivery of the Ru complex from the pore voids to the aqueous solution, was straightforwardly observed via monitoring of the fluorescence band of  $[\text{Ru}(\text{bipy})_3]^{2+}$  dye centered at 610 nm ( $\lambda_{\text{ex}} = 453$  nm) in the aqueous phase.

To investigate the gating properties, in a typical experiment 250  $\mu\text{L}$  of 1 ppm sulfathiazole in PBS was added to 200  $\mu\text{g}$  of **S1-AB**, and the suspension was stirred in order to establish a competition for the antibody between anchored hapten and free sulfathiazole. Release of the reporter was also determined for solutions of **S1-AB** under similar conditions but in the absence of sulfathiazole. The difference in emission in the presence and absence of STZ is displayed in Figure 2, which plots the release behavior. The figure shows that solid **S1-AB** displays a poor release profile versus time (curve a), whereas the same solid in the presence of 1 ppm STZ (curve b) shows clear delivery of the dye: 95% of the maximum release of the entrapped guest was observed after ca. 2 h. Additionally, the figure also shows how release from the capped system can be triggered on command by adding sulfathiazole (1 ppm) at a certain time (curve c). These experiments demonstrate the real possibility of controlling the cargo delivery in water by use of the antigen for which the antibody capping the mesopores is selective.

Additionally, delivery from **S1-AB** as a function of the concentration of the molecular trigger (sulfathiazole) was studied, and the results are illustrated in Figure 3. It can be seen that concentrations as low as 100 ppb sulfathiazole were able to start to uncage the mesopores. The figure also shows that the delivered amount of cargo is proportional to the sulfathiazole concentration, displaying a typical noncompetitive immunoassay response curve in agreement with an uncapping protocol due

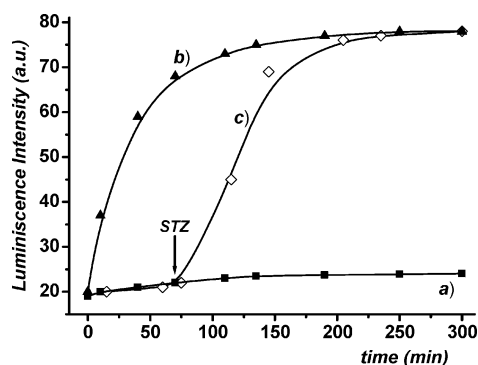


**Figure 2.** Kinetic release of  $[\text{Ru}(\text{bipy})_3]^{2+}$  dye from solid **S1-AB** in the absence (a) and presence (b) of 1 ppm sulfathiazole in aqueous PBS (pH 7.5). A third curve (c) shows the release profile of  $[\text{Ru}(\text{bipy})_3]^{2+}$  complex from **S1-AB** in PBS (pH 7.5) until  $t = 70$  min (indicated by the arrow in the figure), when suddenly sulfathiazole (1 ppm) is added to the solution.

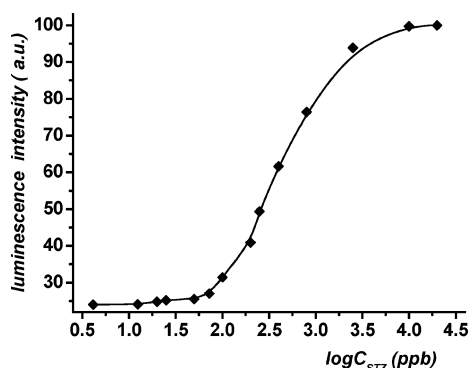


**Figure 3.** Relative percentage of released  $[\text{Ru}(\text{bipy})_3]^{2+}$  dye from **S1-AB** as a function of the concentration of sulfathiazole in PBS (pH 7.5) after 2 h of reaction. The amount of released dye was determined through the emission band ( $\lambda_{\text{em}} = 610$  nm) of the  $[\text{Ru}(\text{bipy})_3]^{2+}$  dye in the solution ( $\lambda_{\text{ex}} = 453$  nm).

to a displacement of the antibody as indicated in Scheme 1.<sup>22</sup> Typically the maximum percentage of dye delivery from **S1** in the presence of STZ was over 50–60% of the loaded dye.

**Selective Delivery.** One of the potential advantages of using antibodies as capping groups is the development of highly selective key-in-lock gating systems. For instance, it is well-known that antibodies can identify and bind only to their unique antigen in mixtures containing a number of different molecules. In order to investigate selectivity in the opening protocol, dye delivery from **S1-AB** was tested in the presence of other molecules very similar to sulfathiazole; that is, a set of sulfonamides (see Supporting Information for the structures). The uncapping ability of these closely related molecules (at 1 ppm concentration) is shown in Figure 4, which plots the fluorescence of the dye released from the SMPS **S1-AB** in the

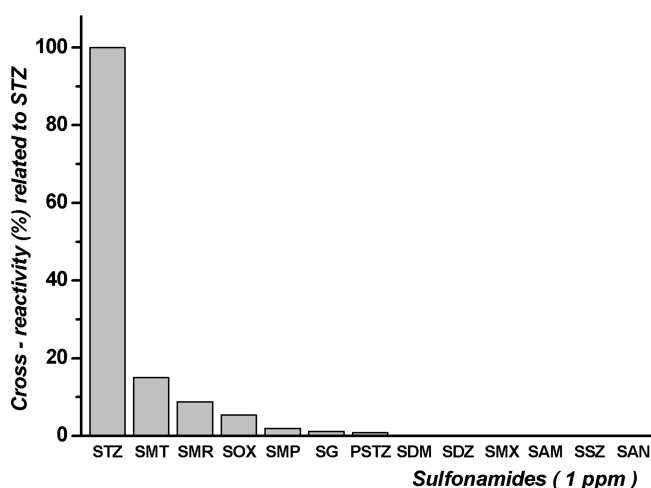


**Figure 4.** Relative release of  $[\text{Ru}(\text{bipy})_3]^{2+}$  from **S1-AB** in the presence of 1 ppm of certain molecules (sulfonamides) in PBS (pH 7.5) after 2 h of reaction. From left to right: sulfathiazole (STZ), sulfamethazole (SMT), sulfamerazine (SMR), sulfisoxazole (SOX), sulfamethoxypyridazine (SMP), sulfaguandine (SG),  $N^4$ -phthalylsulfathiazole (PSTZ), sulfadimethoxine (SDM), sulfadiazine (SDZ), sulfamethoxazole (SMX), sulfacetamide (SAM), sulfasalazine (SSZ), and sulfanilamide (SAN). The structures of these sulfonamides used in the cross-reactivity studies are shown in Supporting Information.

presence of different sulfonamides. A very selective uncapping with sulfathiazole was detected, where only the sulfonamides sulfamethazole (SMT) and sulfamerazine (SMR) show certain cross-reactivity with **S1-AB**.<sup>23</sup>

In addition to these delivery studies with **S1-AB**, further control experiments were carried out with solids **S2** and **S3** in order to evaluate the effect of the anchored hapten on the selective delivery process. Both solids **S2** and **S3** contain the ruthenium dye in the mesopores. Solid **S2** does not have any additional functionalization; **S3** contains amino moieties on the external surface (see Supporting Information for details). As stated above, due to the presence also of an amino group in sulfathiazole, some kind of interaction between the polyamines anchored on **S3** and the antibody was expected.

Aqueous suspensions at pH 7.5 of solids **S2** and **S3** alone showed fast dye release; however, dye delivery was strongly inhibited when **S2** was in the presence of the antibody due to an unspecific adsorption process of the antibody on the surface of **S2**, most likely through interactions with the silanol groups on the SMPS. Most importantly, the addition of sulfathiazole to this **S2-AB** material resulted in no cargo delivery even when large amounts of sulfathiazole were added (up to 50 ppm). In relation to **S3**, addition of the antibody to this solid resulted in the preparation of solid **S3-AB** (analogous to **S1-AB**). The gating properties of this new solid were studied in 250  $\mu\text{L}$  of a solution containing PBS and 200  $\mu\text{g}$  of **S3-AB**, and the release behavior as a function of time in the presence and absence of STZ is displayed in Figure 5 (left). The figure shows that solid **S3-AB** displays a rather important release in the absence of sulfathiazole (curve a) in contrast with the low delivery of the dye observed for **S1-AB** (see Figure 2 curve a). This different behavior is most likely due to much poorer interaction of the

(22) Additionally, although this report deals primarily with the demonstration that it is possible to develop controlled delivery systems using antibody-capped mesoporous nanocontainers, the fact that cargo delivery is proportional to sulfathiazole (antigen) concentration opens the possibility of developing novel label-free immunoassay paradigms where the properties of the reporter (the cargo) could easily be selected at will. Using this concept, further analytical-oriented studies will be carried out in due course. Also the development of displacement one-step analytical formats is very promising because this immunoassay type usually shows higher sensitivity than the corresponding competitive format. See, for instance, González-Techera, A.; Vanrell, L.; Last, J.; Hammock, B. D.; González-Sapienza, G. *Anal. Chem.* **2007**, *79*, 7799–7806.

(23) Although this first example shows a relatively high selective trigger of the cargo delivery, it is important to note that even more selective systems could be prepared using monoclonal antibodies or genetically engineered antibodies. See, for instance, Liddell, E. *Antibodies*. Chapter 8 in *The Immunoassay Handbook*, 3th ed.; Elsevier: Amsterdam, 2005.

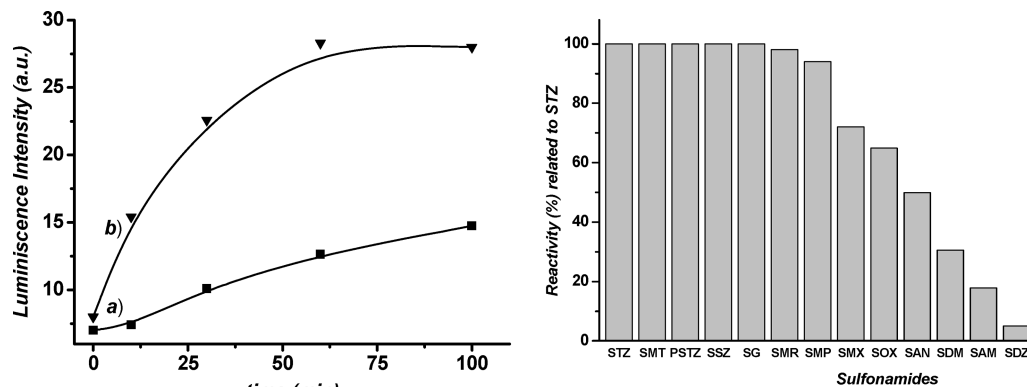


**Figure 5.** (Left) Kinetic release of [Ru(bipy)<sub>3</sub>]<sup>2+</sup> dye from solid **S3-AB** in the absence (a) and presence (b) of 1 ppm sulfathiazole in PBS (pH 7.5). (Right) Relative release of [Ru(bipy)<sub>3</sub>]<sup>2+</sup> from **S3-AB** in the presence of 0.5 ppm of certain sulfonamides (see Supporting Information for structures) in PBS (pH 7.5) after 2 h of reaction.

antibody with the polyamines in **S3-AB** than with the hapten anchored on **S1-AB**. Additionally, from Figure 5 (left) it is also apparent that the presence of sulfathiazole (1 ppm) enhances the delivery of the dye from the **S3-AB** solid (curve b). Much more important in terms of selectivity are the results observed when solid **S3-AB** is tested in the presence of a family of sulfonamides. Figure 5 (right) shows the relative release (with respect to STZ) of the dye from **S3-AB** in the presence of a concentration of 0.5 ppm of these chemicals in PBS (pH 7.5). A clear unselective uncapping process, as effective in many cases as that found with sulfathiazole, was observed for most of the molecules tested.<sup>24</sup> This behavior heavily contrasts with that found under similar conditions with the hapten-containing solid **S1-AB** (see Figure 4). The behavior shown by **S2** and **S3** draws attention to the role played by the anchored hapten groups in the gating mechanism; that is, the hapten in **S1** inhibits the unspecific attachment of the antibody on the mesoporous surface (as occurs in **S2**) and allows at the same time a very selective uncapping protocol to take place in the presence of the target antigen (in contrast with **S3**).

## Conclusions

In conclusion, we have demonstrated, as a proof-of-the-concept and for the first time, that the use of antibodies as gatekeepers on the surface of SMPS provides a suitable method for the design of delivery systems able to selectively release

entrapped guests in the presence of target molecules (antigen) to which the antibody binds selectively. It is advisable to note that this paradigm relies on a different approach, not previously used, and therefore it displays new possibilities for modulation that cannot be considered in other systems. In particular, we believe that gated SMPS based on the use of antibodies may be a promising route for the development of custom-made controlled-delivery nanodevices specifically triggered by target molecular guests. The possibility of including this antibody gating protocol on diverse supports, the potential delivery of different cargos, and the opportunity to select antibodies or similar bioreceptors for a countless amount of possible antigens makes this approach highly appealing for a very wide range of delivery applications in different fields.

## Experimental Section

See Supporting Information.

**Acknowledgment.** We express our gratitude to the Spanish Ministerio de Ciencia y Tecnología (Projects CTQ2006-15456-C04-01, CB07/01/2012, CTQ2007-64735-AR07, and MAT2009-14564-C04-01) for their support. E.C. and A. B. are grateful to the Spanish Ministerio de Ciencia e Innovación and to the Polytechnic University of Valencia for a grant.

**Supporting Information Available:** Details of the synthesis and characterization of materials. This material is available free of charge via the Internet at <http://pubs.acs.org>.

JA904456D

(24) It might be important to note that **S3-AB** or similar systems could be suitable for the development of gating systems that could be opened by similar species such as a set of sulfonamides.